

Bell V-280 System Identification: Application of JIO Methodology for Hover Model Identification

Caitlin S. Berrigan
V-280 Control Law Engineer
Bell
Fort Worth, Texas, USA

Mark J. S. Lopez
Aerospace Engineer
Technology Development
Directorate
CCDC Aviation & Missile Center
Moffett Field, CA, USA

Paul Ruckel
V-280 IPT Control Law Manager
Bell
Fort Worth, Texas, USA

J.V.R. Prasad
Professor and Associate Director
of VLRCOE
School of Aerospace Engineering
Georgia Institute of Technology
Atlanta, GA, USA

ABSTRACT

With the growing complexity of aerospace vehicles, highly coupled redundant flight control surfaces are becoming standard practice. For such vehicles, traditional System Identification (SID) methods, may not accurately capture the individual contributions of effectors to the vehicle bare-airframe response. For the Bell V-280 in a hover configuration, this work used standard SID and the Joint Input-Output (JIO) method to obtain the control power of highly correlated control effectors. The methodology was demonstrated using a high-fidelity hardware-in-the-loop simulation in the V-280 System Integration Lab (SIL), where the identification results can be compared with the known simulation model.

NOTATION

p	Roll rate
r	Reference vector
y	Output vector
δ_A	Actuator of effector bare-airframe input vector
δ_{Ain}	Directly injected bare-airframe input vector
δ_s	Stick or inceptor input vector
DCP	Differential Collective Pitch
JIO	Joint Input-Output (Method)

INTRODUCTION

The rotorcraft industry has long-recognized System Identification (SID) as an important part of fly-by-wire control law development. Using SID in early flight testing can reduce control law development risks and costs associated with in-flight optimization and handling qualities testing. SID methods are also valuable when trying to improve the correlation between flight test data and physics-based flight dynamics models. For traditional pilot-applied stick inputs, current SID tools can extract the aircraft flight dynamic model. However, they may not be able to differentiate the contributions from highly correlated control effectors. For tiltrotors such as the Bell V-280 Valor, flight conditions with highly correlated effectors require a more sophisticated SID approach to determine the control effectiveness of each effector. To address this challenge, the U.S. Army Combat Capabilities Development Command Aviation & Missile Center Technology Development Directorate (CCDC AvMC TDD) and the Universities Space Research Association (USRA) NASA Academic Mission Services (NAMS) are working to incorporate the Joint Input-Output (JIO) method

into their Comprehensive Identification from Frequency Responses (CIFER[®]) SID toolset.

The JIO method has been very successful in recent use for bare-airframe aircraft identification (Refs. 1- 4). This method allows for identification of the individual contributions of each control effector when multiple highly correlated control effectors exist. Results from the JIO method will lead to a more accurate identification for validation of models, control law design, and performance.

Under the Joint Multi-Role Technology Demonstration (JMR TD) program, Bell and CCDC AvMC TDD have collaborated to improve flight control development methods of the Bell V-280 Valor. This work focuses on the collaborative development of methods to identify the contributions of individual control effectors in hover. We anticipate a separate effort to examine control effectors in other configurations.

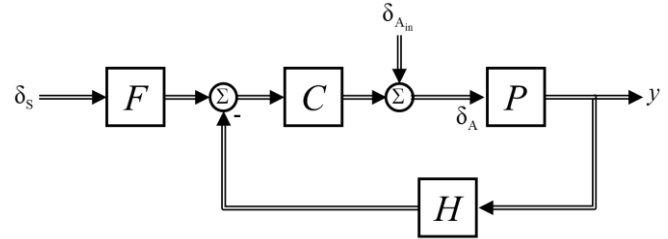
BACKGROUND

Aerospace applications often require the identification of multi-input/multi-output (MIMO) systems, such as a MIMO bare-airframe aircraft model. A non-parametric frequency-response matrix (of the different input-output pairs of a MIMO system) is necessary for determining a parametric model structure. Transfer-function and state-space model identification also rely on using frequency-response identification techniques (Ref. 5). A frequency-response matrix may also be desirable to validate parametric models identified using other frequency or time-domain identification methods (e.g., Maximum Likelihood Estimate or Output-Error Method) (Ref. 6). Many times, inputs to these MIMO systems cannot be independently excited and produce off-axis or secondary inputs that are correlated with the primary input. For example, aircraft with mechanical mixers (such as an aileron-rudder interconnect) cannot move one control surface without moving the other. Aircraft with control allocation to multiple bare-airframe inputs, or unstable aircraft that cannot be excited without a feedback control system engaged are other examples. For these examples, partially correlated inputs are accurately addressed using a multi-input conditioning direct method approach (Ref. 5). However, when the inputs to multiple control effectors are highly correlated to a single response, the separate contributions of each effector are difficult to distinguish using traditional system identification methods. In such cases, an accurate frequency-response model of the MIMO system cannot be determined without some additional processing.

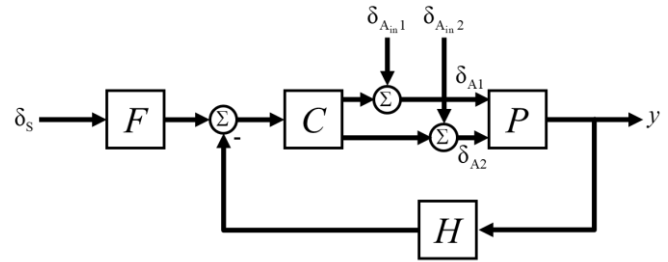
Highly Correlated Inputs

Consider the generic block diagram in Fig. 1, with MIMO bare-airframe P , controller (including control allocation /mixer) C , sensor model and feedback H , and feed-forward/prefilter F . The pilot stick or inceptor inputs are denoted by vector δ_s , bare-airframe actuator or effector inputs by vector δ_A , and bare-airframe outputs by vector y . Inputs

δ_{Ain} may also be summed directly into the bare-airframe inputs. Any number of signal elements in the bare-aircraft input vector δ_A may be highly correlated; for example, in Fig.-1 the control allocation can simultaneously use multiple redundant inputs δ_{A1} and δ_{A2} to generate an aircraft moment, thus δ_{A1} and δ_{A2} would be highly correlated.



a. Multi-Input Multi-Output



b. Two-Input One-Output

Figure 1. Generic closed-loop block diagram.

Several methods are available to deal with highly correlated inputs (Refs. 5 and 7 attempt to de-correlate inputs, and Ref. 8 indirectly identifies a closed-loop system). An approach called the Joint Input-Output (JIO) method has recently shown great success. The JIO method considers the inputs and outputs of the bare-airframe jointly as outputs to an intermediate reference input. The JIO Method was first proposed by Akaike (Ref. 9) to mitigate noise, but has been used recently for inflow model identification (Refs. 10 and 11) and bare-airframe aircraft identification (Refs. 1-4). While bare airframe identification using the JIO Method has been used successfully for full-scale manned fixed-wing vehicles (Refs. 1 and 2), application to Vertical Takeoff and Landing (VTOL) vehicles has been limited to simulations or sub-scale and unmanned vehicles (Refs. 3 and 4).

SYSTEM IDENTIFICATION METHODOLOGY

Methodology

Referring to Fig. 1, the system identification goal is to determine a bare-airframe frequency response matrix

$P = [y/\delta_A]$. That bare-airframe response matrix is the basis for identifying parametric models (transfer-function and state-space models), which can then provide important information such as the control derivatives or effectiveness. This frequency-domain approach (Ref. 5) invokes the JIO method as an additional post-processing step to obtain the bare-airframe response to individual control effectors (Ref. 3). The closed-loop vehicle is excited using frequency sweeps of the control inceptors/effectors to smoothly excite a broad range of aircraft response frequencies. The time history signals for the sweep, control effectors, and aircraft response are recorded, then transformed into the frequency domain using CIFER[®] (Ref. 5).

The JIO method computes the bare-airframe frequency response matrix by first computing responses with respect to reference signals r . Herein, r becomes the external sweep commands. The actuator-to-reference frequency response matrix $[\delta_A/r]$ and the output-to-reference frequency response matrix $[y/r]$ are computed. Subsequently, at each frequency ω , the bare-airframe response matrix is simply the product of the actuator-to-frequency response matrix inverse with the output-to-reference frequency response matrix:

$$\left[\frac{y}{\delta_A}(j\omega) \right] = \left[\frac{y}{r}(j\omega) \right] \left[\frac{\delta_A}{r}(j\omega) \right]^{-1} \quad (1)$$

In scalar form, Eq. 1 can be thought of simply as a type of chain rule calculation of y/δ_A .

For the present work, it is important to define “actuator” versus “effector”. The JIO method can be applied to individual hydraulic actuators or can be applied at the effector level (e.g., rotor swashplate collective, rotor swashplate longitudinal / lateral cyclic). From a flight control law perspective, the V-280 control effectors (e.g., rotor Differential Collective Pitch (DCP) and rotor lateral cyclic) are of most interest and are used for the JIO method application. In the hover regime, these tiltrotor control methods are somewhat redundant in that either DCP or lateral cyclic can be used to control the vehicle in low speed flight.

While the standard pilot stick inceptor inputs (δ_s) are excellent for obtaining frequency responses of the “effective” bare-airframe $\hat{P} = P \cdot C$, an issue arises for redundant control inputs. In such cases, the number of pilot stick inceptor inputs δ_s is less than the number of actuator inputs δ_A . To use the JIO method, the actuator-to-reference frequency response matrix must be invertible $[\delta_A/r]$. Therefore, the matrix must be square (the number of reference signals r must equal the number of actuator signals δ_A). Alternatively, it is possible to exercise an approach that uses “engineering test commands” to directly sum with the control allocation outputs. The sum is sent directly to the actuators as δ_{Ain} shown in Figure 1. The engineering test command approach relies on knowing the

exact location of the vehicle excitation signal. The excitation signal is an automated sinusoidal sweep (automated sweep), which excites a known frequency band of interest over a duration of 90s. The automated sweep can be either summed in at the pilot inceptor or desired effector directly. In SIL testing, it was found that a combination of inceptor input, δ_s , and direct effector automated sweep, δ_{Ain} , provided the best results for determining the effector control powers. The approach also minimized the number of additional test points compared to standard SID methods. Consequently, the reference signal r (in Fig. 1) is always chosen as the automated sweep, which can be δ_s or δ_{Ain} .

V-280 SYSTEM IDENTIFICATION

Aircraft Description

The V-280 SIL represents the V-280 aircraft, shown in Fig. 2. The V-280 is Bell’s next generation tiltrotor designed for a Future Long-Range Assault Aircraft (FLRAA) program of record. In the 24 months of flight test, Team Valor has accumulated over 100 hours of flight time and 200 operating hours (Ref. 12). The V-280 has exceeded 300 knots, without sacrificing range, payload capacity, or flying qualities.



Figure 2. V-280 in VTOL Mode flight.

The V-280’s two engines are fixed horizontally on the wingtips, while the rotor pylons are actuated to allow for Vertical Take-Off and Landing (VTOL), hover, and forward flight. In the VTOL configuration, the aircraft uses a combination of rotor collective and cyclic inputs for control authority. During conversion and cruise mode, control transitions to flaperons and ruddervators. The overall control system is well harmonized, yet presents a case where redundant control effectors are in use for major portions of the flight envelope.

As stated earlier, lateral control in hover is an example of redundant control allocation. The pilot’s lateral stick displacement results in both DCP and symmetric lateral cyclic at both rotor heads. The proportions of DCP and lateral cyclic are determined by a fixed-ratio control allocation strategy that is based on the pilot’s lateral cyclic stick displacement. For

helicopter-mode lateral control, the V-280 control laws will always command both DCP and lateral cyclic, meaning they are always fully correlated.

SIL Test Execution

The V-280 SIL integrates both real hardware (flight control computer, avionics, pilot inceptors, and actuators) and a 6 DOF math model which is based on Generic TiltRotor (GTR) for aircraft response and includes modeling for other dynamic components including engine, drive train, and sensor models. The GTR flight loads are applied to the aircraft actuators through load actuator. In the SIL, frequency sweeps were performed in three different ways: manual piloted stick inceptor input, automated sweep at the inceptor input, and lastly, automated sweep at the effector. A sample time history of an automated lateral sweep input is shown in Fig. 3 with the simulated aircraft roll rate response. The sweep command at the inceptor is shown in blue, the control effector signals (DCP and lateral cyclic at the rotor) are shown in red, and the aircraft roll rate response is shown in green. As can be seen from the time histories, both lateral control effector signals (DCP and lateral cyclic) have very similar frequency content at any point in time, indicating that the controls are highly correlated.

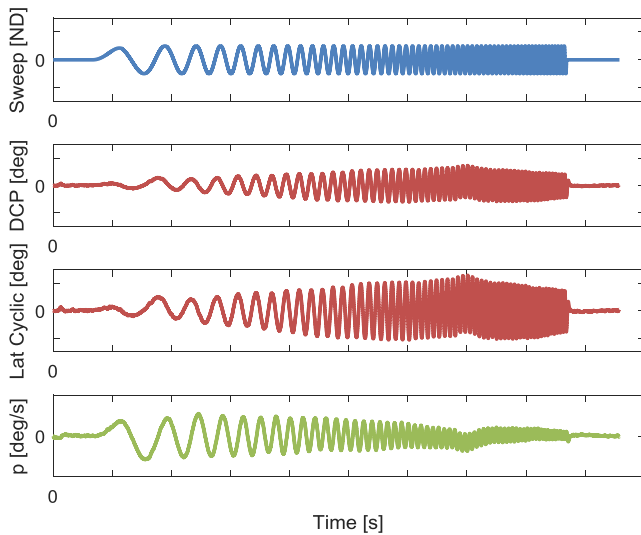


Figure 3. Automated lateral stick sweep in hover shows that DCP and Lateral Cyclic (at the rotor head) are highly correlated.

As there are two highly correlated control effectors (DCP and lateral cyclic), the JIO method requires two sets of linearly independent frequency sweeps. The lateral stick sweep is a standard frequency sweep used in routine system identification procedures: from Fig 1b-BlockDiagram a sweep input at δ_s is allocated through C to both DCP (δ_{A1}) and lateral cyclic (δ_{A2}). To obtain the second sweep, which enables JIO to be used, a frequency sweep is sent directly to the DCP effector as $\delta_{Ain,1}$ of Fig. 1b. Here, the bare-airframe responds (P), but the response is feedback (H) and allocated

through (C), resulting in both DCP (δ_{A1}) and lateral cyclic (δ_{A2}) becoming correlated. The resulting time histories for the DCP effector sweep are shown in Fig. 4. Similar to the lateral stick sweep, the DCP effector sweep results in correlation between the DCP effector and the lateral cyclic control effector. The correlation can be observed in Fig. 4 by the very similar frequency content of the effectors at any point in time.

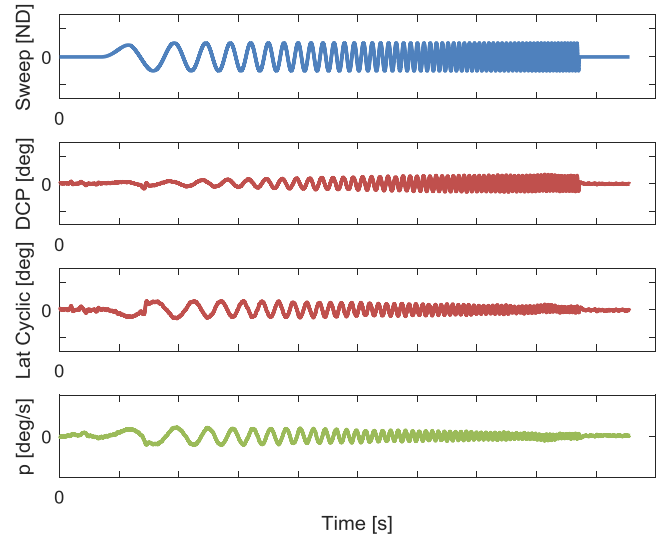


Figure 4. Automated DCP effector sweep in hover shows that DCP and Lateral Cyclic (at the rotor head) are highly correlated.

The correlation in Fig. 4 can be quantitatively assessed using the cross-control coherence of lateral cyclic to DCP, as shown in Fig. 5. The cross-control coherence is shown for both the lateral inceptor sweeps and DCP effector sweeps. The cross-control coherence is nearly 1 for the majority of the identified frequency range, indicating that DCP and lateral cyclic are completely correlated. Tischler, (Ref. 5), indicates that MIMO conditioning using the direct (standard) method can accurately extract the MIMO frequency response matrix when the cross-control coherence is less than 0.5

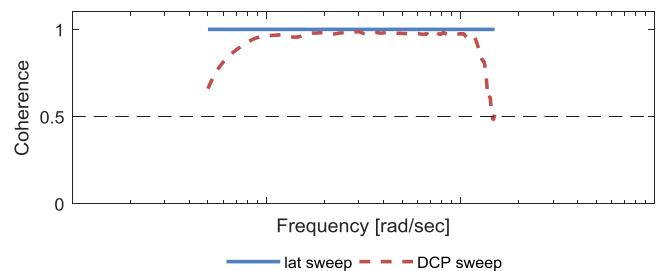


Figure 5. Lateral cyclic to DCP coherence is close to 1 for the entire frequency range, indicating complete cross-control correlation between the effectors.

The qualitative and quantitative measures indicate very high DCP and lateral cyclic correlation. Thus, the JIO process can instead be used to accurately obtain frequency responses with respect to individual control effectors.

Frequency Response Identification

The lateral stick and DCP effector frequency sweep time histories were processed within CEFER[®] utilizing the JIO methodology to obtain frequency responses. Measured signals included pilot and effector inputs, as well as vehicle response. A sample roll rate frequency response to DCP, is shown in Fig. 6, where both piloted and automated sweeps are compared.

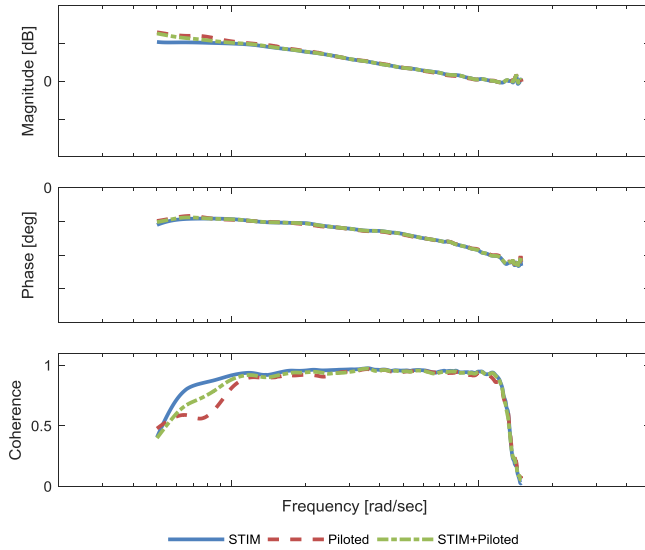


Figure 6. Roll rate to DCP frequency response for automated versus piloted frequency sweeps.

JIO results were obtained from automated sweeps (labeled as “STIM”) from piloted sweeps (labeled as “Piloted”), and also by combining (concatenating) both automated and piloted sweeps (“labeled as “STIM+Piloted”). The primary difference between each data set can be observed at the lower-mid end of the frequency range, where there are differences in coherence (and thus data quality). While the standard guidance is to use piloted sweeps (Ref. 5), here it was found that the automated sweeps tend to give the best coherence. The primary reason for this is believed to be associated with the biomechanics of the cockpit – sometimes the pilots were found to rush through mid-frequencies. This resulted in a lower quality sweep. The recommendation is to fly both automated and manual piloted sweeps, but only use two data records, selected for the highest quality. This combination provides the richer content from the piloted inputs, while improving consistency in the mid frequency range.

In addition to the JIO methodology, the frequency sweep time histories were also processed with the traditional SISO technique (assuming all response is due to one effector at a

time and neglecting the other). The roll rate frequency response to each lateral effector (DCP and lat cyclic), is shown in Fig. 7. This figure shows both the JIO computed frequency response and the SISO frequency responses for the cases where one input is neglected. Responses are shown for both DCP and lateral cyclic effector inputs. The difference between the JIO and SISO frequency response for DCP is negligible, indicating that the SISO solution is satisfactory for DCP in that particular sweep. However, the JIO frequency response for lateral cyclic is much smaller in magnitude than the SISO calculated response. This is expected, given that DCP has a much larger contribution to roll in hover and cannot be ignored. Thus, the SISO solution yields incorrect results as it cannot split the control power between the two fully-correlated effectors and should not be used for lateral cyclic.

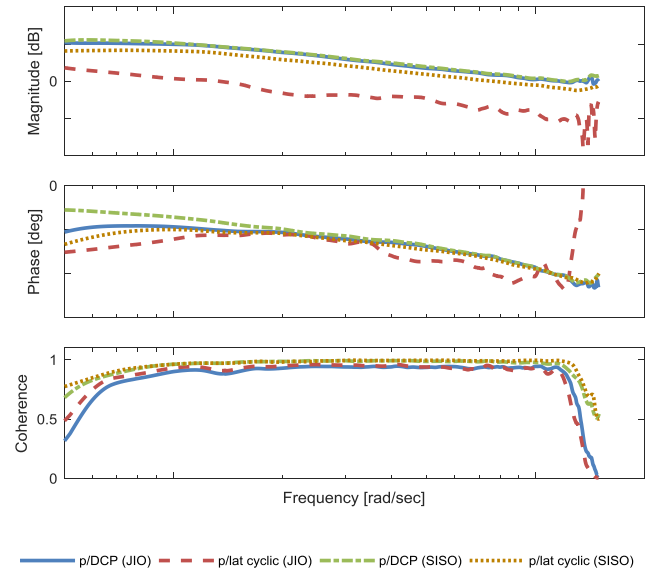


Figure 7. DCP and Lateral Cyclic to roll rate frequency response.

Transfer Function Identification

Once frequency responses have been identified, a low-order transfer function approximation can be identified to determine effective stability and control derivatives. For a hovering vehicle, a low-order 2nd over 3rd order transfer function for roll rate can be derived in terms of stability and control derivatives (Ref. 13), with an effective time delay added to account for higher-order rotor-inflow dynamics:

$$\frac{p(s)}{\delta(s)} = \frac{L_{\delta} \left[s^2 + \left(-Y_v + \left(\frac{Y_{\delta}}{L_{\delta}} \right) L_v \right) s \right]}{s^3 + (-Y_v - L_p) s^2 + Y_v L_p s - g L_v} e^{-\tau s} \quad (2)$$

Here, δ is a control effector (e.g. DCP or lateral cyclic) and L_{δ} is the associated roll control derivative. The 2nd over 3rd order transfer function provides a good overall approximation of

the pertinent aircraft derivatives over a wide frequency range. However, identification of the actual derivatives requires additional considerations. Thus, while the 2nd over 3rd order approximations can be valuable, a simpler approximation is desired to obtain the control derivatives directly. This can be done by assuming that the frequency range being identified corresponds only to the control derivative, and that all other stability derivatives and corresponding dynamic modes act at sufficiently low frequency such that they can be neglected (i.e., can assume that $Y_v=L_v=L_p=0$). Under this assumption, the roll transfer function simplifies to a 0th over 1st, k/s type of approximation:

$$\frac{p(s)}{\delta(s)} = \frac{L_\delta[s^2]}{s^3} e^{-\tau s} = \frac{L_\delta}{s} e^{-\tau s} \quad (3)$$

The k/s approximation provides the associated control derivative directly as $L_\delta = k$. This high-frequency approximation will provide the most accurate initial estimate of the control derivative, under the assumption that all other derivatives and modes have sufficient frequency separation from where the control derivative is effective. Also, due to the simplistic nature of the approximation with only 2 parameters (L_δ and τ), the identification process is very robust to any local perturbations in the frequency response due to noise or random error.

The k/s low order approximation is used to estimate the control derivatives from the roll rate frequency responses. Transfer function coefficients are identified in CIFER[®], and the control derivatives can be directly identified as the leading numerator coefficient, under the assumption that all applicability requirements have been met.

A sample frequency response for DCP to roll rate is shown in Fig. 8, which compares the JIO frequency responses identified from the SIL relative to the identified transfer function approximations. A k/s transfer function, indicated as “TF ID” is identified on the basis of only high frequency portions of the frequency sweep. The identified transfer function has excellent agreement with the SIL data, having a cost function $J < 50$ for the applicable frequency range. The $J < 50$ cost function indicates that the identified transfer function and SIL data are nearly indistinguishable (Ref. 5).

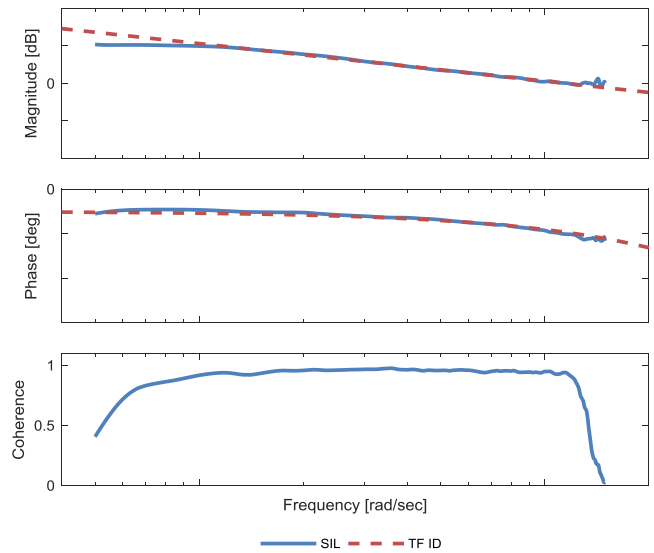


Figure 8. DCP to roll rate frequency response from JIO and low order transfer function approximation.

Similarly, a frequency response for roll rate to lateral cyclic is shown in Fig. 9, which compares the JIO frequency responses identified from the SIL relative to the identified transfer function approximations. A k/s transfer function (high frequency only) is identified and has excellent agreement with the SIL data, with a cost functions $J < 50$ for the applicable frequency ranges. This result indicates that the identified transfer function and SIL data are nearly indistinguishable (Ref. 5).

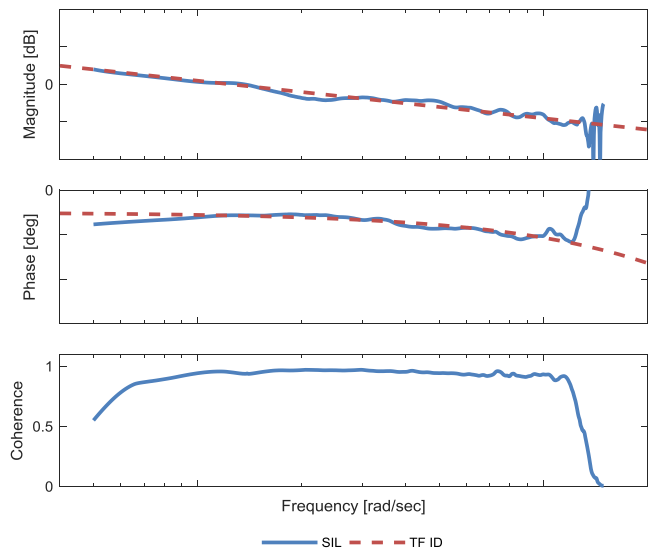


Figure 9. Lateral Cyclic to roll rate frequency response from JIO and low order transfer function approximation.

While determination of the roll control derivatives and control effectiveness is important to the control allocation design, the primary parameter of interest is actually the ratio of control effectiveness for the two control effectors (DCP at the rotor and Lateral Cyclic at the rotor). One way to directly obtain the ratio of control effectiveness is to compute the ratio of p/DCP and p/(lat cyclic) frequency responses. At high frequency, this frequency response ratio simplifies to:

$$\frac{\left(\frac{p(s)}{DCP(s)}\right)}{\left(\frac{p(s)}{lat\ cyclic(s)}\right)} = \frac{\left(\frac{L_{DCP}}{s} e^{-\tau_{DCP}s}\right)}{\left(\frac{L_{lat\ cyclic}}{s} e^{-\tau_{lat\ cyclic}s}\right)} = \frac{L_{DCP}}{L_{lat\ cyclic}} e^{(-\tau_{DCP} + \tau_{lat\ cyclic})s} \quad (4)$$

Thus, at high frequency, the ratio of p/DCP and p/(lat cyclic) directly provides the ratio $L_{DCP} / L_{lat\ cyclic}$ which is the ratio of the control effectiveness of DCP to lat cyclic. The frequency response ratio of p/DCP and p/(lat cyclic) is shown in Fig. 10, along with the “high frequency” identified transfer function from Eq. 4.

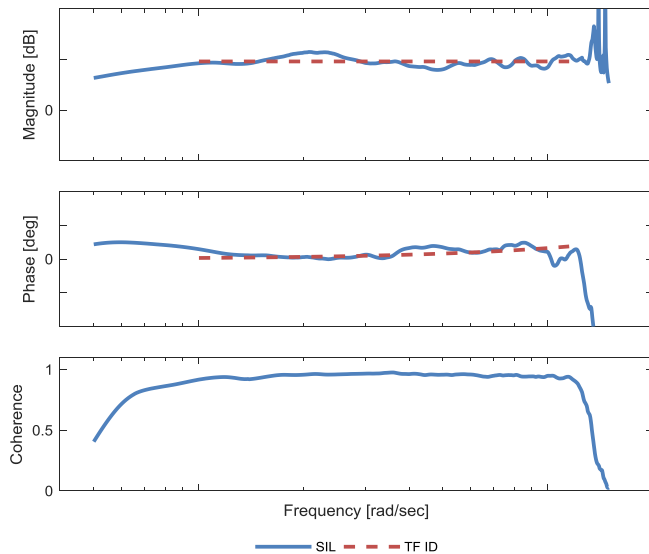


Figure 10. Ratio of p/DCP and p/(lateral cyclic) frequency response from JIO and transfer function approximation.

Comparison of Control Effectiveness

Both DCP and Lateral Cyclic Transfer functions are identified for all roll rate frequency responses. In addition, Transfer functions are identified from both JIO and SISO approximation frequency responses.

The identified control derivatives (control effectiveness) from each identified transfer function are shown as bar-chart representations in Fig. 11. Identified control derivatives are also compared with Bell’s linear perturbation model which is considered here as the known truth for comparison.

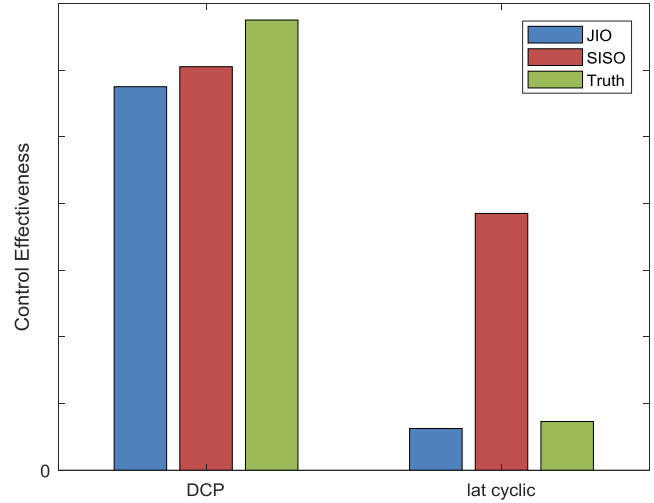


Figure 11. Identified roll control effectiveness for DCP and lateral cyclic.

Comparison of DCP control effectiveness, both identified results and truth results from the perturbation model, are in good agreement, giving confidence to identified values from both JIO and SISO approximation methods.

Comparison of lateral cyclic control effectiveness indicates that the identified results from the SISO approximation are much higher compared with the JIO identified control effectiveness. The JIO identified control effectiveness is in good agreement with the results from the perturbation models, giving confidence that the JIO identified control effectiveness is correct. This indicates that the SISO approximation produces acceptable results for the identification of DCP control effectiveness but, should not be used for lateral cyclic. More importantly, these results indicate that the JIO frequency responses and identified control effectiveness is an accurate and viable method for identifying control effectiveness for the V-280 in hover.

Finally, a comparison of the ratio of control effectiveness of DCP / (lateral cyclic) can be produced by simply dividing the control effectiveness (control derivatives) of DCP by lateral cyclic. The results of the control effectiveness ratios are displayed in bar-chart form in Fig. 12.

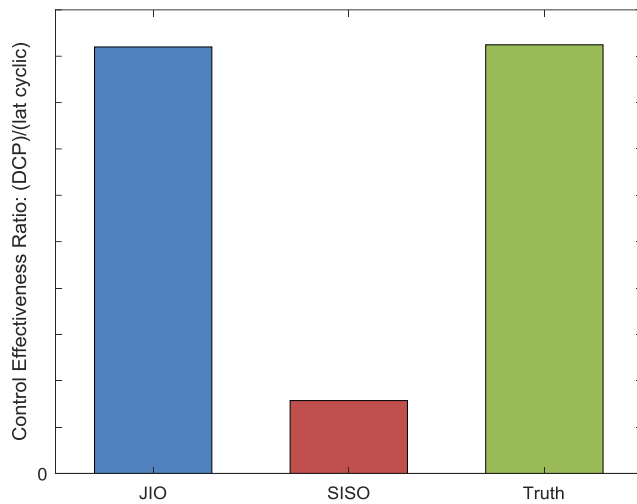


Figure 12. Ratio of roll control effectiveness for DCP/(lat cyclic).

As expected, the JIO results are in good agreement with the truth results from the linear perturbation model. The SISO approximations significantly under predict the control effectiveness ratio and should not be used.

CONCLUSIONS

For tiltrotors such as the Bell V-280 Valor, flight conditions with highly correlated effectors require a more sophisticated SID approach to determine the control effectiveness of each effector. Key elements of this work include:

- 1) The JIO methodology accurately extracted frequency responses from correlated effectors.
- 2) Control derivatives (control effectiveness) can be directly identified from frequency responses using high frequency, low order transfer function approximations.
- 3) A combination of standard sweeps from the piloted stick with additional effector sweeps provided the best quality data for performing system identification with the JIO methodology.
- 4) To minimize flight test time, only one of the correlated effectors needs to be individually swept per axis if the inceptor is also swept.

ACKNOWLEDGMENTS

The success of this joint project is due to the efforts and support of many contributors beyond the authors of this paper, thank you V-280 team and CCDC AvMC TDD. In addition, the authors would like to thank the pilots from Bell for safely gathering excellent quality data.

REFERENCES

1. Knapp, M. E., Berger, T., Tischler, M. B., and Cotting, M. C., "Development of a Full Flight Envelope Flight Identified F-16 Simulation Model," AIAA Paper 2018-0525, January 2018, doi: 10.2514/6.2017-1550.
2. Berger, T., Tischler, M. B., Knapp, M. E., and Lopez, M. J., "Identification of Multi-Input Systems in the Presence of Highly Correlated Inputs," AIAA Journal of Guidance, Control, and Dynamics, June 27, 2018.
3. Berger, T., Tischler, M. B., Knapp, M. E., and Lopez, M. J., "Identification of Multi-Input Systems in the Presence of Highly Correlated Inputs," presented at the Atmospheric Flight Mechanics Conference at AIAA SciTech, San Diego, CA, January 7-11, 2019.
4. Lopez, M. J. S., Tischler, M. B., Juhasz, O., Gong, A., and Sanders, F.S., "Development of a Reconfigurable Multicopter Flight Dynamics Model from Flight Data Using System Identification," presented at the Vertical Flight Society 8th Biennial Autonomous VTOL Technical Meeting, Mesa, AZ, January 29-31, 2019.
5. Tischler, M. B. and Remple, R. K., *Aircraft and Rotorcraft System Identification: Engineering Methods and Flight Test Examples Second Edition*, AIAA 2012, doi: 10.2514/4.868207.
6. Morelli, E. and Klein, V., *Aircraft System Identification – Theory and Practice, 2nd Edition*, Sunflyte Enterprises, 2016.
7. Jung, S., Shim, D. H., and Kim, E.-T., "Helicopter Dynamic Model Identification by Conditional Attitude Hold Logic," AIAA Paper 2017-1251, January 2017, , doi: 10.2514/6.2017-1251.
8. Forssell, U. and Ljung., L., "Closed-Loop Identification Revisited," *Automatica*, 25(7): 1215-1241, July 1999, doi: 10.1016/S0005-1098(99)00022-9.
9. Akaike, H., "Some Problems in the Application of the Cross-Spectral Method," in *Spectral Analysis of Time Series* (ed. B. Harris), 81-107, John Wiley, New York, 1967.
10. Gennaretti, M., Gori, R., Serafini, J., Cardito, F., and Bernardini, G., "Identification of Rotor Wake Inflow Finite-State Models for Flight Dynamics Simulations," *CAES Aeronautical Journal*, Vol. 8, (1), pp. 209230, March 2017, doi: 10.1007/s13272-016-0235-y.
11. Hersey, S., Celi, R., Juhasz, O., Tischler, M. B., Rand, O., and Khromov, V., "State-Space Inflow Model Identification and Flight Dynamics Coupling for an Advanced Coaxial Rotorcraft Configuration," presented at the American Helicopter Society 73rd Annual Forum, Fort Worth, TX, May 2017.
12. Ehinger, R., McMenemy, M., and Wilson, P., "Bell V-280 Valor: JMR TD Flight Test Update – Year 2," presented at the Vertical Flight Society 75th Annual Forum & Technology Display, Philadelphia, PA, USA,

May 13-16, 2019.

13. McRuer, D. T., Graham, D., and Ashkenas, I., *Aircraft Dynamics and Automatic Control*, Princeton University Press, 1973, doi: 10.1515/9781400855988.